Xiaoping Gao*,
Nannan Tao,
Si Chen,
Liping Wang,
Wei Wu

Tensile-tensile Fatigue Behavior of Multi-axial Warp-knitted Reinforced Composite

DOI: 10.5604/01.3001.0010.7800

Inner Mongolia University of Technology, College of Light Industry and Textile,
Inner Mongolia, Hohhot, 010051, China
* E-mail: gaoxp@imut.edu.cn

Abstract
An experimental study was carried out on the fatigue behaviour of multi-axial warp-knitted fabric composites. Composite samples reinforced with multi-axial warp-knitted fabric/matrix were manufactured by the vacuum-assisted resin transfer moulding method. Tensile-tensile fatigue cycling was carried out at different load levels, and S-N curves, tensile stress-strain curve and stiffness degradation of the multi-axial composite samples were obtained. Finally post-fatigue tensile tests were done at a stress level of 75%, at the stages of 1/3N and 2/3N, and the equivalent residual strength and stiffness degradation were obtained.

Key words: *multi-axial warp-knitted fabric composite, fatigue behavior, S-N curve, equivalent residual strength.*

Introduction

Textile composite materials are widely used in aerospace, marine industries and wind turbine blades [1] due to their excellent strength and stiffness to weight ratio and the lack of yarn undulations which exist in woven fabrics. Multi-axial warp-knitted fabrics (MWFs) are manufactured from multiple layers of straight fiber bundles with different orientations stitched together by a warp knitting procedure [2, 3].This procedure creates a material which is heterogeneous not only at the micro-scale but also at the meso-scale, due to the bundle structure in the layers. This makes them attractive materials for use in high-performance composites.

Most researchers have focused on the mechanical behaviour of composites. In the long-term use of composite material, the stiffness is degraded with the environment and alternative external loading, resulting in the fatigue accumulation and destruction of the material eventually. Thus it is very important to study the fatigue properties of composites. As far as the MWF composite is concerned, the main fatigue damage is matrix cracking, delamination, interface debonding and fiber breakage, which result in a decline in fatigue strength and stiffness [4]. Ivanov [5] investigated the tensile properties of non-crimp 3D orthogonal woven and multi-layer plain weave composites and observed that non-crimp 3D orthogonal woven composites have a significantly higher in-plane strength, failure strain and damage initiation threshold than 2D woven laminated ones. The bending fatigue behaviours of a 3D angle-interlock woven composite, 3D orthogonal woven composite, and 3D braided rectangular composite were investigated through experimental and finite element analysis [6-10], respectively. The tensile-tensile fatigue behavior of a layer-to-layer 3D angle-interlock woven composite was studied [11]. Vallons, et al [12] considered the tensile-tensile fatigue and post-fatigue behaviour of carbon/epoxy non-crimp fabric composites. Karahan et al [13] observed the fatigue tensile behavior of a carbon/epoxy composite reinforced with non-crimp 3D orthogonal woven fabric. The result reveals that the damage development at the early stage of fatigue loading could be characterised by the combination of transversal cracks in the fiber bundles, boundary debonding cracks at the surfaces of fiber bundles transverse to the loading direction, and in local debonding cracks parallel to the sample facings.

In this paper, multi-axial warp-knitted fabrics were used as reinforcement materials, 100 epoxy resins and 30 curing agents as the matrix, and composite samples were manufactured by VARTM. The MWF composites had three kinds of samples, i.e. uniaxial, biaxial and triaxial, which are abbreviated as U, B, T, respectively. The fatigue behaviors of the MWF composite, such as the S-N curve, damage curve and post-fatigue properties were investigated, as well as the fatigue damage of the composite.

Materials and fabrication of composites

Materials

Glass fiber has excellent properties, such as non-burning, high temperature resistance, small moisture absorption, little elongation etc. Multi-axial warp-knitted glass fabrics have the advantages of high orientation, high elastic modulus, good drape and high resistance to delamination. The composite reinforced

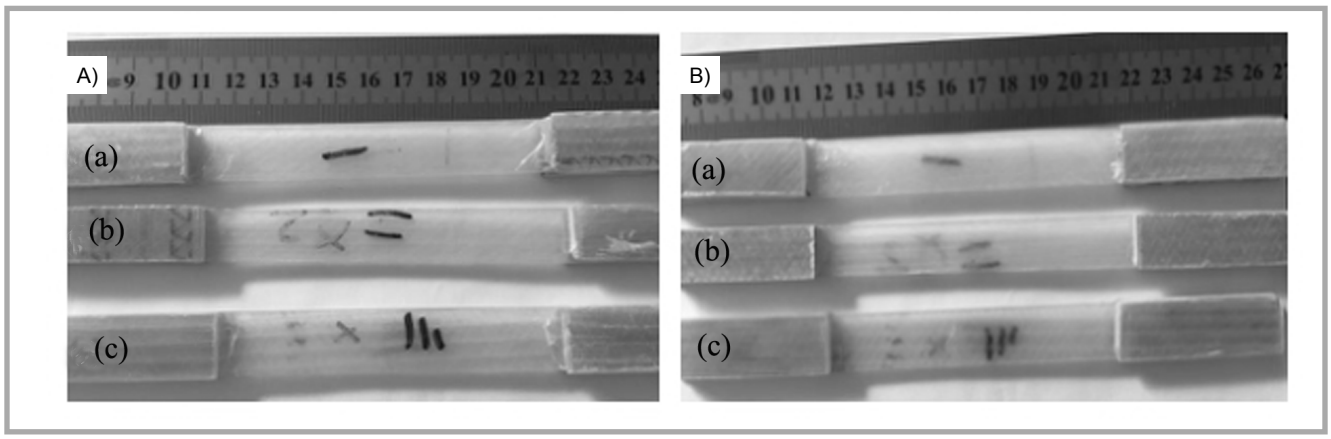

Figure 1. *Fatigue specimens: (A) front, (B) back; (a) uniaxial, (b) biaxial, (c) triaxial.*

with multi-axial warp-knitted fabric has the advantages of stable size, high strength, high stiffness, high yarn utilisation efficiency, anti-stratification and high fiber volume fraction; thus they are widely used in composite manufacturing. The multi-axial warp-knitted fabrics (MWFs) in this paper, manufactured by Taishan fiberglass Inc. (China), were prepared for reinforcement. In this fabric, the glass fibers were alkali free roving, and had good mechanical properties. The surface of the glass fibers were treated with silane coupling agent, which is beneficial to the adhesion between epoxy resin and glass fibers. Glass fiber bundles were used for unidirectional reinforcing, while polyester fibers (the linear density is 83 dtex) were uitilised for knitting the linking part. The mechanical performances of glass fiber are shown in ***Table 1***, and the parameters of the different axial warp-knitted fabrics are shown in ***Table 2***. The fiber directions in the fabric are oriented at 0°, 90° or 45° relative to the machine direction.

Table 1. *Mechanical performance of glass fiber.*

Materials	Density, g/cm³	Elastic modulus, GPa	Fracture strength, GPa	Elongation at break, %	Shear modulus, GPa
Glass fiber	2.56	30	1.56	2.7	28.58

Table 2. *Parameters of different axial warp knitted fabric.*

Fabrics		Fineness, tex	Thickness, mm	Weight, g/m²	Density, bundels/10cm
U	0°	2400	0.58	1134	27
	90°	300		59	20
B	+45°	600	0.6	401	53
	-45°	600		401	53
T	0°	2400	1.08	709	23
	+45°	300		250	50
	-45°	300		250	50

Table 3. *Physical performance of epoxy resin and curing agent.*

	Viscosity, cps	Density, g/cm³	Ignition point
Epoxy resin (2511-1A)	1200	1.1	>150 °C
Curing agent (2511-1BT)	17	0.9	>120 °C

Table 4. *Sizes of different axial composite samples.*

Materials	Cutting direction	Average width, mm	Average thickness, mm	Lay-out of fabric
U	0°	15.27	2.41	Three layers with same direction
B	0°	15.63	2.34	Four layers with same direction
T	0°	15.63	2.34	Three layers with same direction

Composite preparation

The composite plates in this study were prepared with VARTM (vacuum assisted resin transfer moulding). In this process, a flat aluminum plate was used as a mold. The mold surface was cleaned with acetone and coated with a mold release agent. In the first step, fabric layers were stacked in the mold to form plates in such a way as to gain symmetry of the stacking sequence. In the second step, a solution composed of 100 parts mass of epoxy resin (E-2511-1A) and 25 parts mass of a curing agent (2511-1BT) were transferred from a reservoir onto a flat aluminum plate at a vacuum pressure of -0.095 MPa. During the injection, a vacuum of -0.095 MPa was applied in the cavity. The physical performance parameters of the epoxy resin and curing agent are shown in ***Table 3***.

After injection, the mould was transferred to a furnace maintained at 80 °C for 8 h in order to obtain fast curing. Finally the composite plates were cut into narrow strips of 200 (length) × 15 (width) × 2.4 thickness) mm. Three millimeter-thick composite end tabs with dimensions of 50 mm × 15 mm were glued onto the samples to minimise localised damage and to provide better load transfer from the grips to the samples, giving a test length of 100 mm. The composite specimens are shown in ***Figure 1***. A minimum of five samples were tested in the 0° direction for each type of composite. The sizes of different axial composite samples are shown in ***Table 4***.

Mechanical testing

Quasi-static tensile tests

Quasi-static tensile tests of the MWF composites were carried out in the 0° direction according to the ASTM standard D3039-93. The composite samples were

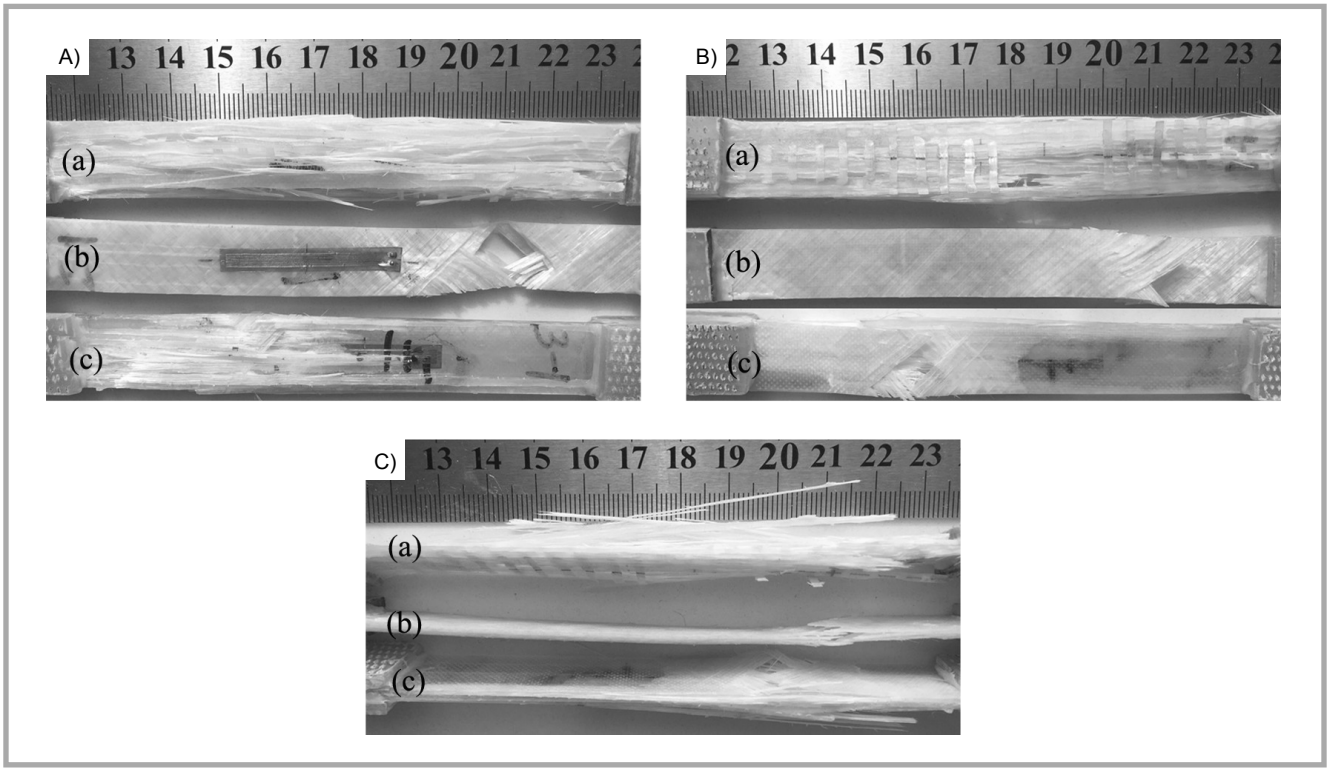

Figure 2. *Fracture morphology of three composite specimens under quasi-static tensile tests: (A) face, (B) back, (C) lateral; (a) uniaxial, (b) biaxial, (c) triaxial.*

tested on a WDW-100J universal testing machine (Jinan Meisite Company, China). To register the displacement in both the length and width directions during the test, extensometers with dimensions of 30 × 12.5 mm were attached to the specimen. The test speed was 2 mm/min, and the strain was continuously measured with an extensometer.

Fiber volume fraction

The fiber volume fractions were obtained by applying a burning method according to the ASTM D3171-15 standard. The specimen was burned in a muffle furnace at 450-650 °C, and the epoxy was evaporated. The fiber volume fraction was then calculated by weighing the specimen and residue, as shown in ***Equation (1)***. The volume fraction of fibers V_f was calculated according to the following formula:

$$V_f = \frac{\rho_m W_f}{\rho_f W_m + \rho_m W_f} \qquad (1)$$

Where, W_f – weight of the fiber, g; W_m – weight of the matrix, g; ρ_f – density of the fiber, g/cm³; ρ_m – density of the matrix, g/cm³.

The equivalent strength and modulus of the composite specimens were normalised to a fiber volume fraction of 45% with respect to ***Equations (2)*** and ***(3)***.

The equivalent strength:

$$F^{ut}{}_{normal}(45\%) = F^{ut} \times 45\% / V_f \qquad (2)$$

The equivalent modulus:

$$E_{normal}(45\%) = E_0 \times 45\% / V_f \qquad (3)$$

Where, F^{ut} – tensile strength, $F^{ut}{}_{normal}$ – equivalent strength, E_0 – elastic modulus, E_{normal} – equivalent modulus.

The stress-strain behaviour of MWF composites under quasi-static tensile testing is shown and compared in ***Table 5***. The fracture morphology of three different composite specimens under quasi-static tensile testing is shown in ***Figure 2***.

From ***Table 5***, it can be clearly seen that the tensile strength, equivalent strength, elastic modulus and equivalent modulus of the uniaxial composite specimen have the largest values. As shown in ***Figure 2***, at the fracture location of the samples the delamination phenomenon appears, and the fracture is relatively neat. Yarns of the uniaxial samples are fractured only in the 0° direction, and those of the biaxial samples are delamination fractured in the ±45° direction. Yarns of the triaxial samples are tensile fractured in the 0° direction and delamination fractured in the ±45° direction. The relationships between the tensile strength and equivalent strength, and between the elastic modulus and equivalent modulus of the composite specimens are obtained with ***Equations (2)*** and ***(3)***. With respect to ***Tables 2*** and ***5***, it can be concluded that the tensile strength and tensile modulus of the composite are dependent on the fineness and weight of the fiber bundles.

Fatigue test

A tensile-tensile fatigue test was carried out according to GB/T 16779-2008. The tensile-tensile fatigue behaviour of the MWF composites was tested on the American MTS Landmark system. The test adopted the pattern of stress control, as shown in ***Figure 3***.

Table 5. *Tensile properties of three composites.*

Material	F^{ut}, MPa	E_0, GPa	V_f, %	$F^{ut}{}_{normal}$, MPa	E_{normal}, GPa	Strains, %
U	670.64	9.07	56.60	533.19	7.21	7.41
B	109.59	2.47	48.37	101.95	2.30	16.63
T	373.45	6.93	56.19	299.08	5.55	6.29

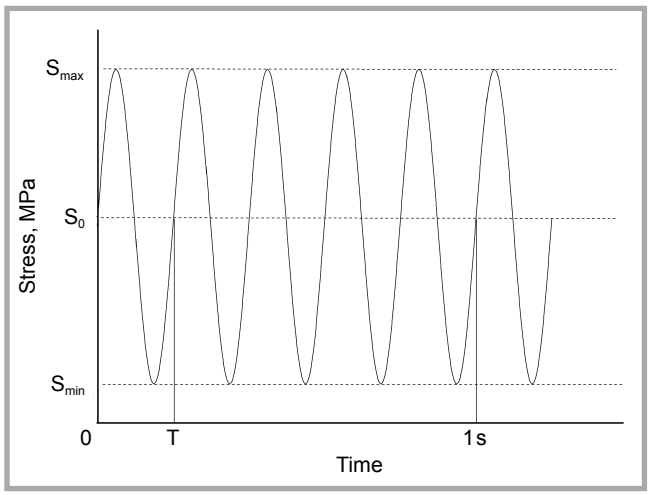

Figure 3. Sinusoidal load.

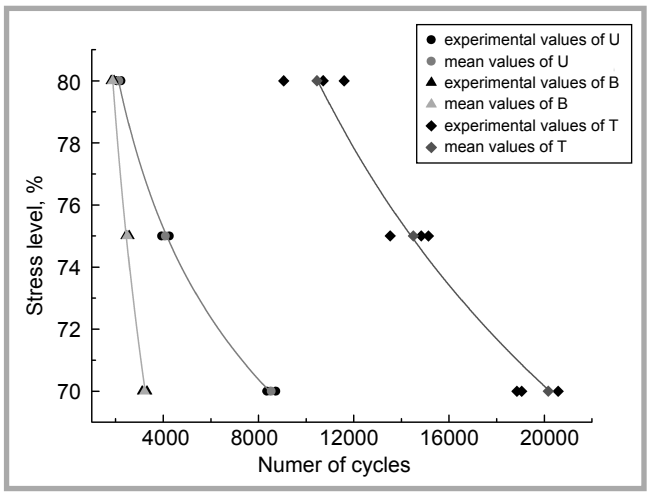

Figure 4. S-N curve of MWF composite samples.

Specific experiment parameters are as follows:

1) Stress ratio R (ratio of the minimum stress to the maximum stress in one cycle): 0.1;
2) Frequency: 5Hz;
3) Test environment state: 20 °C, dry state.
4) Stress levels S_{max}/σ_{ult} (ratio of the maximum stress applied in one cycle to the ultimate static tensile stress): 80%, 75% and 70%.

Three different composite samples were selected for the tensile-tensile fatigue test, and three levels of stress were selected for each kind of sample. The tensile strength as well as the maximum and minimum stress at different levels of stress are shown in ***Table 6***.

Residual strength test of post-fatigue

Firstly a tensile-tensile fatigue test under specified cycles at a certain stress level were carried out. Secondly the resulting specimens were then subjected to quasi-static experiments. Lastly the residual strength of the composite samples was tested. The conditions of the residual strength test at a stress level of 75% under cycles of 1/3N and 2/3N are shown in ***Table 7***. The sample under a fatigue loading of 1/3N at a 75% stress level is referred to as sample-A and the sample under a fatigue loading of 2/3N at a 75% stress level is referred to as sample-B for simplification in the following sections.

Results and analysis

S-N curve

The fatigue life is an important index to characterise a material's fatigue behaviour. Fatigue life (N) is the number of cycles of alternating stress that a sample is subjected to under certain a certain level (S) of stress. An S-N curve of the multi-axial warp-knitted composite at the stress levels (80%, 75% and 70%) is shown in ***Figure 4***.

Figure 4 shows that the fatigue cycles decrease with the increasing of the stress level. The fatigue life of the composite under the same level of stress was as follows: $N_T > N_U > N_B$. The greater the number of fatigue cycles, the stronger the fatigue resistance the samples have. This phenomenon is associated with the structure of samples and the cutting direction. In this paper, the uniaxial fabric only has yarn whose layout is in the 0° direction, and the yarn density in the 0° direction is 1.35 times that of 90° direction yarn, with the samples being cut along the 0° direction, which will increase the fatigue resistance of the uniaxial samples. As far as the biaxial composite sample is concerned, the specimens are not cut along the direction of yarns i.e. the ±45° yarns are not subjected directly to alternating stress; thus the fatigue resistance of the biaxial sample is lower. As for the triaxial composite samples, they are cut along the 0° direction, and yarns in the ±45° direction can also absorb part of the load, thus the fatigue resistance of the triaxial samples is the best at the same stress level.

Table 6. *Tensile strength under different stress levels.*

Sample	Loading direction	Stress level	F^{ut}, MPa	S_{max}, MPa	S_{min}, MPa
U	0°	80%	670.64	536.51	53.51
		75%		502.98	50.98
		70%		469.45	46.95
B	0°	80%	109.59	87.67	8.77
		75%		82.19	8.22
		70%		76.71	7.67
T	0°	80%	373.45	298.76	29.88
		75%		280.09	28.01
		70%		261.42	26.14

Stiffness degradation

Stiffness is the ability of the material to resist elastic deformation under the action of stress. In the process of bending fatigue, the stiffness of the composite will be gradually degraded under cyclic stress loading. The degradation of stiffness can be reflected by the modulus variation of the material. In this paper, the modulus variation was normalised to the index which is the ratio of modulus E which can be obtained in tensile fatigue to the initial modulus E_0. As shown in ***Figure 5***, E/E_0 decreases quickly, then varies smoothly, and finally decreases quickly with the increasing of the number of cycles. With respect to the variation in E/E_0, the variation in the material modulus can be divided into three stages (as can be seen from ***Figure 5***). Matrix cracks occur in the first stage, and the

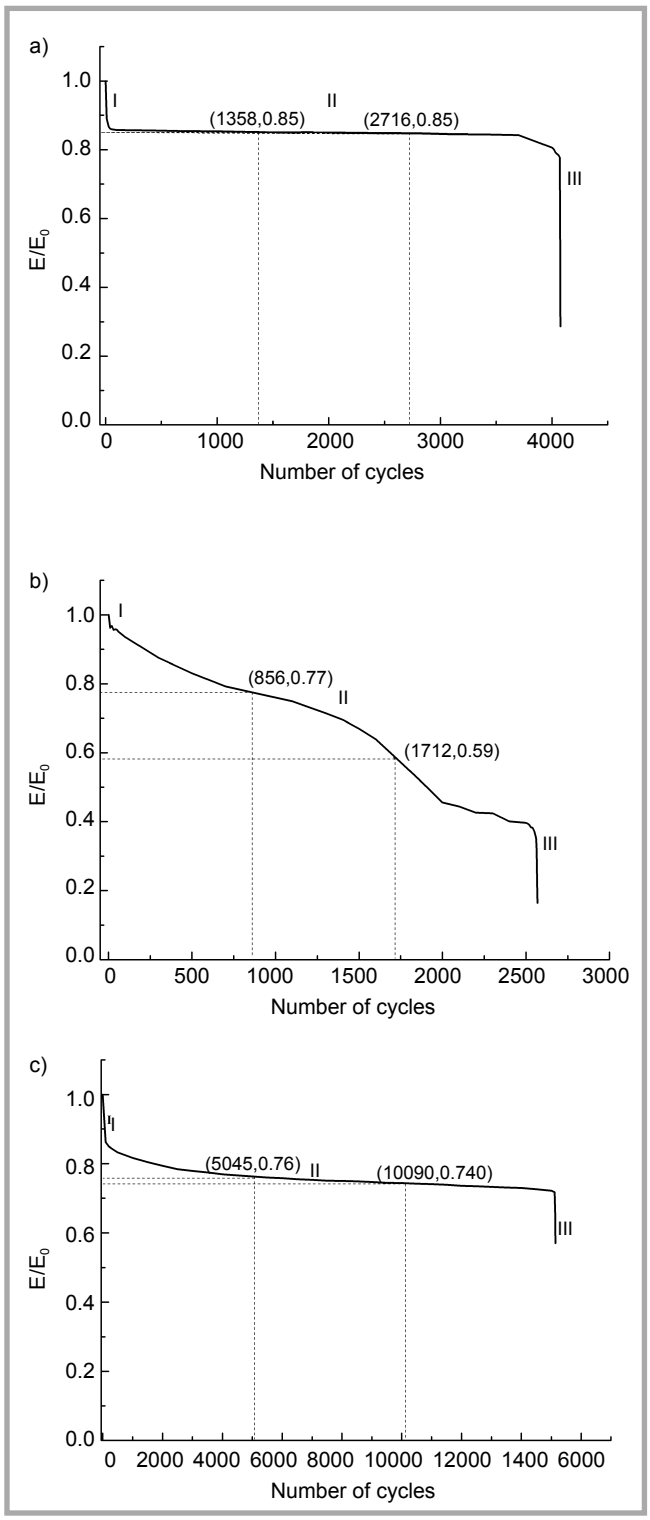

Figure 5. Degradation curve of modulus: (a) uniaxial, (b) biaxial, (c) triaxial.

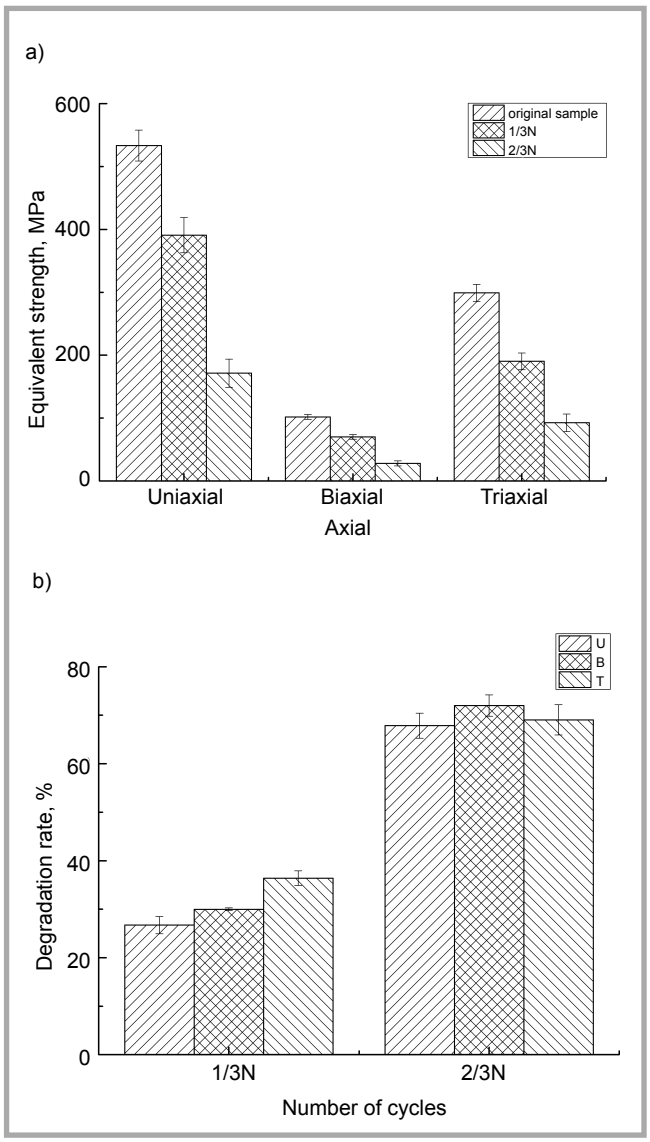

Figure 6. Equivalent strength and degradation rate of different composite samples: (a) comparison of equivalent strength, (b) comparison of degradation rate.

Table 7. Conditions of residual strength test of post-fatigue.

Sample	Stress level	Cycles, N	1/3N	2/3N
U	75%	4074	1358	2716
B		2570	856	1713
T		15136	5045	10090

modulus of the sample decreases rapidly. The modulus variation of the uniaxial and triaxial samples is relatively stable in the second stage, and debonding between the matrix and fibers occurs slowly. However, the modulus of biaxial samples decreases dramatically. Lastly the fiber breaks instantaneously and the sample eventually fails.

Residual strength

The behaviour of the composite is influenced by the fibre volume fraction. The tensile strength and residual strength after cycles of 1/3N and 2/3N at a 75% stress level were normalised to the equivalent strength according to ***Equation (2)*** for comparison. The equivalent strength and degradation rate of different composite samples are shown in ***Figure 6***.

It can be concluded that the equivalent residual strength of the composite will decrease with the increasing of loading cycles. However, the degradation rate will increase with the increasing of loading cycles, indicating that the degree of

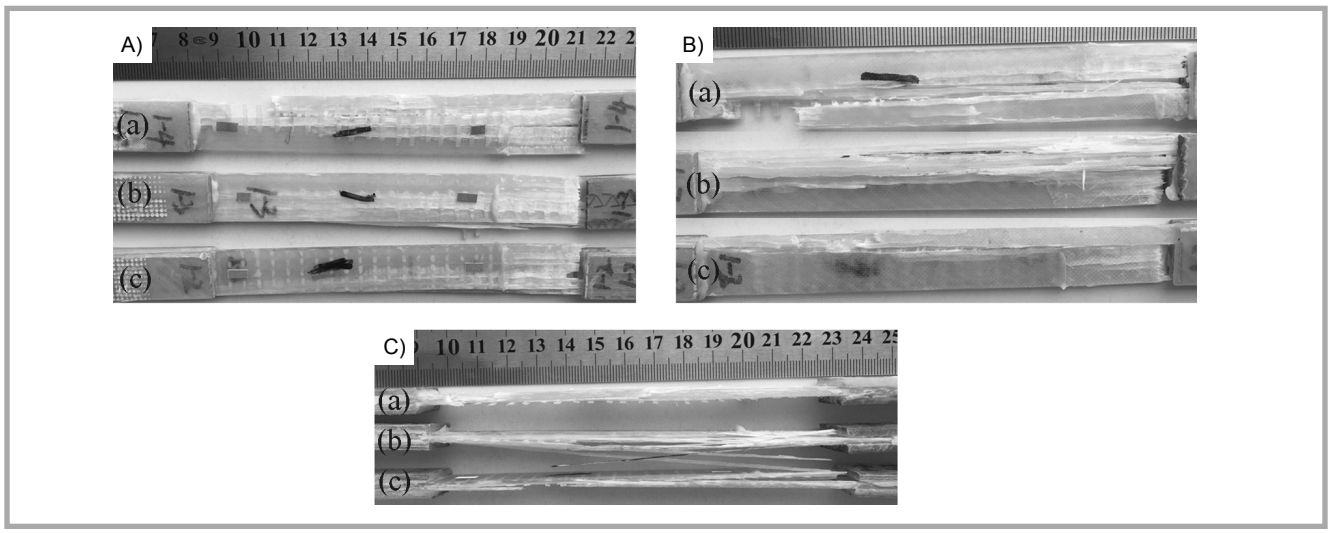

Figure 7. *Fracture morphology of uniaxial samples under fatigue loading: (A) face, (B) back, (C) lateral, (a)70%, (b) 75%, (c) 80%.*

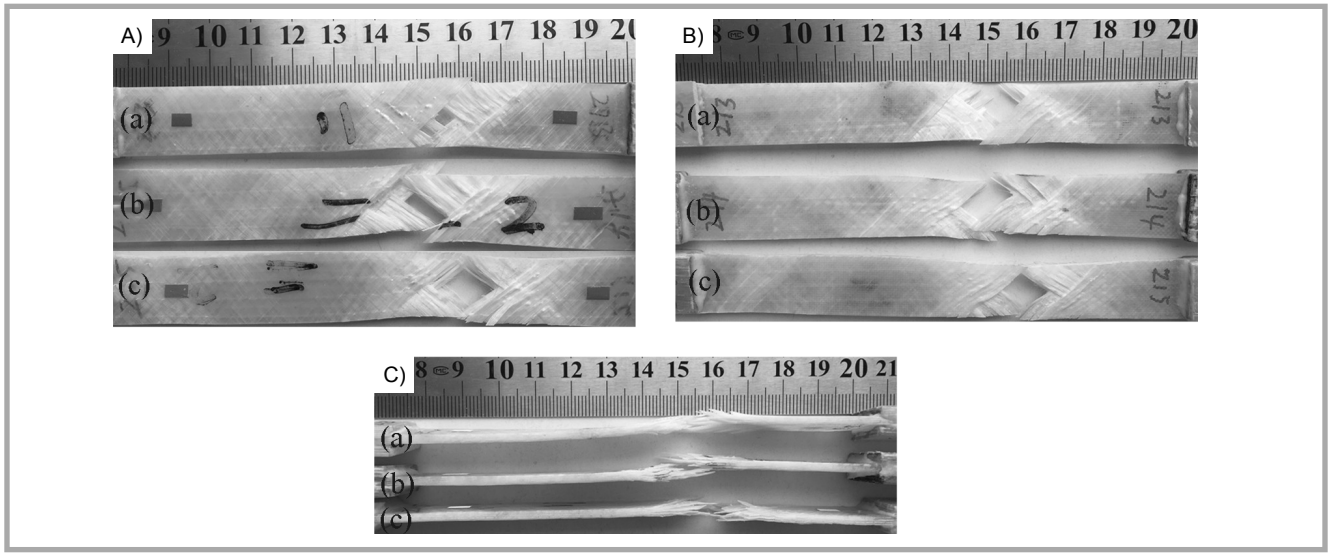

Figure 8. *Fracture morphology of biaxial specimens under fatigue loading: (A) face, (B) back, (C) lateral, (a)70%, (b) 75%, (c) 80%.*

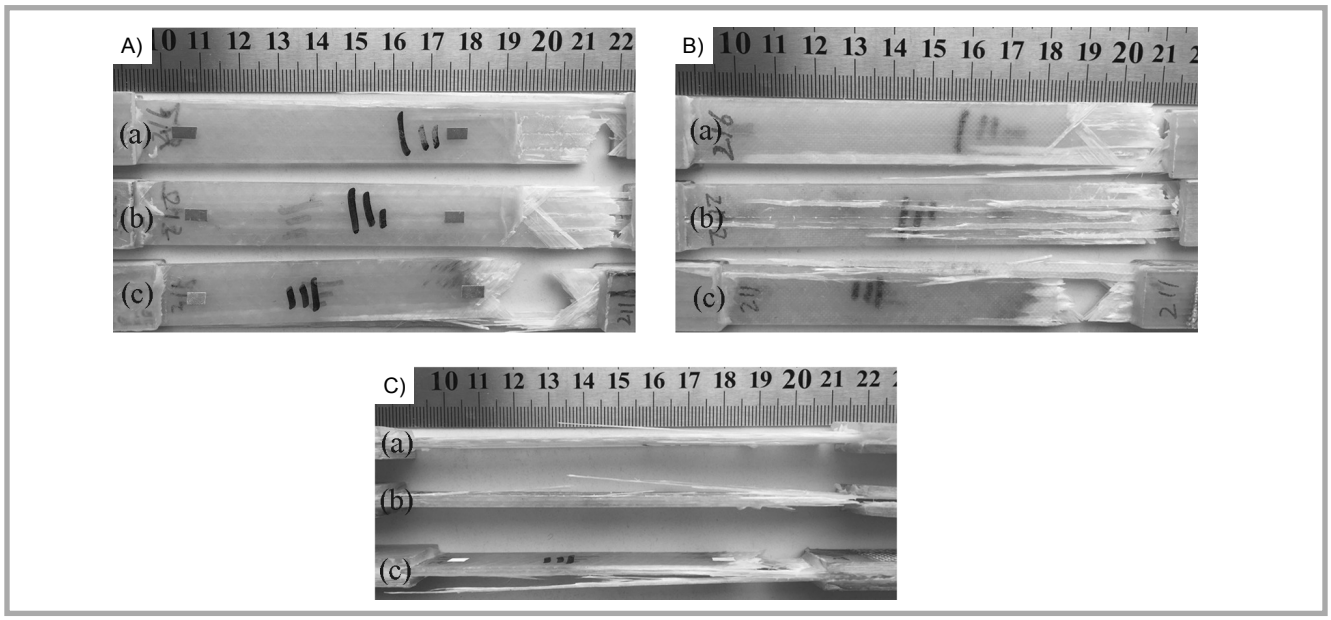

Figure 9. *Fracture morphology of triaxial samples under fatigue loading: (A) face, (B) back, (C) lateral, (a)70%, (b) 75%, (c) 80%.*

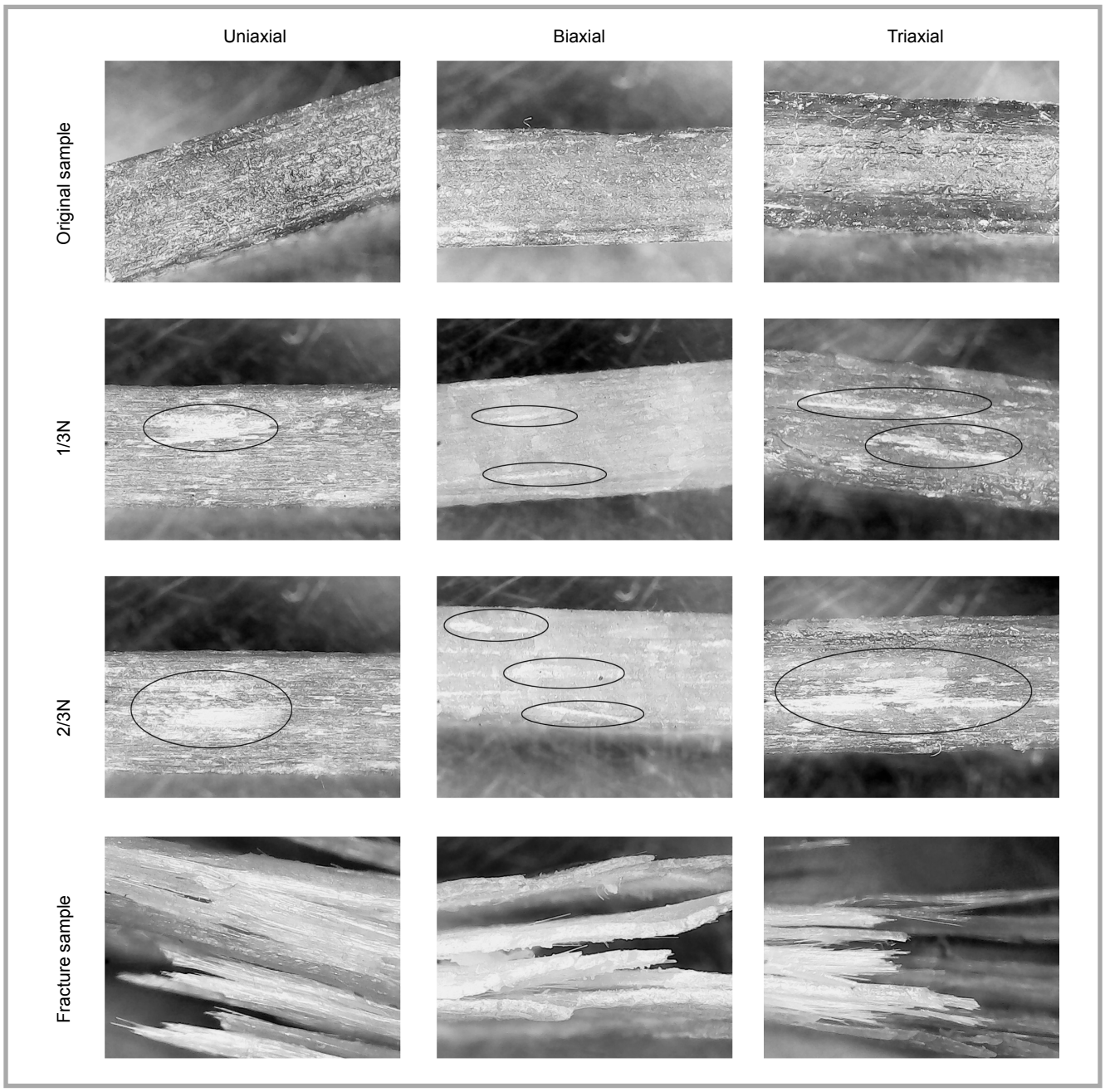

Figure 10. *Lateral view of MWF composite samples.*

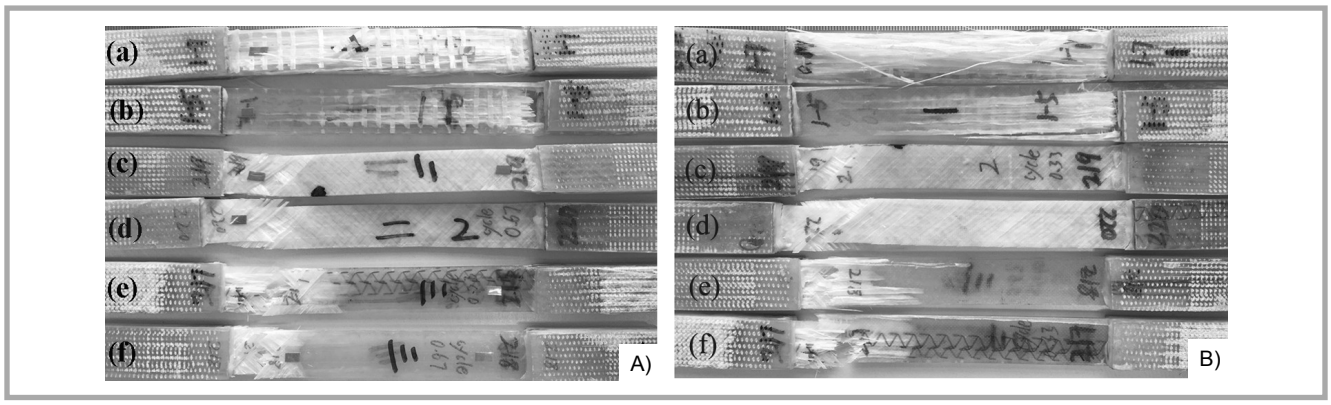

Figure 11. *Fracture morphologies of the specimen after a post-fatigue test. (A) front, (B) back. (a) uniaxial, stress level: 75%, N: 1358, (b) uniaxial, stress level: 75%, N: 2716; (c) biaxial, stress level: 75%, N: 856, (d) biaxial, stress level:75%, N: 1713; (e) triaxial, stress level: 75%, N: 5045, (f) triaxial, stress level: 75%, N: 10090.*

damage increased with an increase in the number of cycles. As for sample-A, the relationship between the degradation rates of the different composites is as follows: T > B > U. As for sample-B, the relationship between the degradation rates of the composites is as follows: B > T > U, which is inverse to the variation in E/E_0.

Fracture morphology

The fracture morphologies of different composite samples under fatigue loading are shown in ***Figures 7-9***.

On the basis of the fracture morphology, it can be concluded that the failure modes of the composite include matrix cracking, interface debonding between fibers and the matrix, and fiber fracture. As for the uniaxial and triaxial composite specimen, serious fracture occurred with the increasing of the stress level.

As shown in ***Figures 7-9***, we can also ascertain that the composite specimens have serious debonding between the fiber and matrix. In order to verify this phenomenon, the damaged surfaces of the composite specimens were observed by digital microscope, as shown in ***Figure 10***.

Figure 10 shows a lateral view of the specimen. White cracks due to debonding between the fiber and matrix occurred at the fracture site, and extended along the longitudinal direction of the samples. By comparing the lateral morphologies of sample-A and sample-B, it can be seen that the area and number of cracks at the 2/3N stage are significantly larger than equivalent ones at the 1/3N stage, which indicated that the sample damage is dependent on the number of cycles.

Fracture morphologies of the composite specimens after a number of fatigue cycles are shown in ***Figure 11***.

Figure 11 shows that the cross sections of the fracture surface are orderly, where almost no fibers were pulled out. As for the uniaxial and triaxial specimen, there is remarkable debonding between the fiber and matrix, which are attributed to specimen fracture and delamination between the fiber and matrix.

Conslusions

The tensile-tensile fatigue behaviour of a MWF composite was studied. The quasi-static tensile test, tensile-tensile fatigue test and residual strength test after post-fatigue were experimentally executed at three stress levels. The S-N curve, tensile stress-strain curves, the variation in the modulus, the variation in the equivalent strength, the degradation of stiffness, and the fracture morphology of the samples were analysed.

The results show that the fatigue cycles decreased with the increasing of stress levels in the specimen, and that the tiraxial specimen has the maximum fatigue life, while the biaxial specimen has the minimal fatigue life at the same level of stress. The inelasticity hysteresis loops of stress-strain in the fatigue process can be used to explain the strain hysteresis of the composite. The area of the hysteresis loop will result in an increasing in damage energy and cumulative damage.

The variation in the modulus indicates that the failure of the composite can be divided into three stages, i.e. matrix cracks, debonding between the resin and fiber, and instantaneous fiber fracture. The crucial stage is the debonding between the fiber and resin; and thus the bonding strength of the composite can be increased by improving the adhesion between fibers and the matrix.

The residual strength of the composite specimen could be decreased, but the stiffness degradation, which has an inverse relationship to E/E_0, would increase with the increasing of the number of cycles in relation to the equivalent strength and stiffness degradation.

The main failure modes include matrix cracking, debonding between the fiber and matrix, and fiber fracture during tensile fatigue according to the fracture morphology of specimen. Post-fatigue failure is attributed to debonding between the fiber and matrix after 1/3N and 2/3N at the 75% stress level. The material's stiffness is degenerated gradually with the increasing of the number of cycles, which is the result of crack evolution.

Acknowledgements

This work was supported by The National Natural Science Foundation of China (Grant No. 11462016 and No. 51765051), The Natural Science Foundation of Inner Mongolia under grant No.2017MS0102.

References

1. Stolyarov O, Quadflieg T, Gries T. Effects of fabric structures on the tensile properties of warp-knitted fabrics used as concrete reinforcements. *Text Res J.* 2015; 85: 1934-1945.
2. Loendersloot R, Lomov SV Akkerman R. Carbon composites based on multiaxial multiply stitched preforms. *Compos Part A-Appl S.* 2006; 37:103-113.
3. Lomov SV, Belov EB, Bischoff T. Carbon composites based on multiaxial multiply stitched preforms. Part 1. Geometry of the preform. *Compos Part A-Appl. S.* 2002; 33: 1171-1183.
4. Shokrieh MM, Lessard LB. Progressive Fatigue Damage Modeling of Composite Materials, Part I: Modeling. *J Compos Mater.* 2000; 34: 1056-1080.
5. Ivanov DS, Lomov DS, Stepan V, Bogdanovich, AE, Karahan M,Verpoest I. A comparative study of tensile properties of non-crimp 3D orthogonal weave and multi-layer plain weave E-glass composites. Part 2: Comprehensive experimental results. *Compos Part A-Appl. S.* 2009; 40: 1144-1157.
6. Sun BZ, Yao Y, Jin LM, Gu BH. Finite element analyses of stress distributions of three-dimensional angle-interlock woven composite subjected to three-point bending cyclic loading. *J Text I.* 2013; 104: 1186-1194.
7. Jin LM, Jin BC, Sun BZ, Gu BH. Comparisons of static bending and fatigue damage between 3D angle-interlock and 3D orthogonal woven composites. *J Reinf Plast Comp.* 2012; 31: 935-945.
8. Jin LM, Hu H, Sun BZ, Gu BH. Three-point bending fatigue behavior of 3D angle-interlock woven composite. *J Compos Mater.* 2012; 46: 883-894.
9. Sun BZ, Niu ZL, Jin LM, Zhang Y, Gu BH. Experimental investigation and numerical simulation of three-point bending fatigue of 3D orthogonal woven composite. *J Tex I.* 2012; 103: 1312-1327.
10. Zhao Q, Jin LM, Jiang LL, Zhang Y, Sun BZ, Gu BH. Experimental characterizations of bending fatigue of a four-step 3-D braided rectangular composite under different stress levels. *J Reinf Plast Comp.* 2011; 30: 1571-1582.
11. Jin L, et al., Tension–tension fatigue behavior of layer-to-layer 3-D angle-interlock woven composites. *Mater Chem Phys.* 2013; 140: 183-190.
12. Vallons K, Lomov SV, Verpoest I. Fatigue and post-fatigue behaviour of carbon/epoxy non-crimp fabric composites. *Compos Part A-Appl. S.* 2009; 40: 251-259.
13. Karahan M, et al., Fatigue tensile behavior of carbon/epoxy composite reinforced with non-crimp 3D orthogonal woven fabric. *Compos Sci Technol.* 2011; 71: 1961-1972.

Received 21.03.2017 Reviewed 18.08.2017